Aerospace Science and Technology 86 (2019) 775–781

Contents lists available at ScienceDirect

Aerospace Science and Technology

www.elsevier.com/locate/aescte

Experimental study of flame characteristics of ethylene and its mixture with methane and hydrogen in supersonic combustor

Fengquan Zhong [a,b,*,1], Liuwei Cheng [a,1], Hongbin Gu [a], Xinyu Zhang [a,b]

[a] State Key Laboratory of High Temperature Gas Dynamics, Institute of Mechanics, Chinese Academy of Sciences, Beijing 100190, China
[b] School of Engineering Science, University of Chinese Academy of Sciences, Beijing 100049, China

ARTICLE INFO

Article history:
Received 7 May 2018
Received in revised form 18 January 2019
Accepted 18 January 2019
Available online 28 January 2019

Keywords:
Supersonic combustor
Hydrocarbon
Mixture fuel
Flame structure
Ignition

ABSTRACT

In this paper, flame characteristics of ethylene and its mixture with methane and hydrogen in process of ignition in a Mach 2.5 supersonic model combustor are studied. Development of flame structure is visualized with CH* chemiluminescence images recorded by high-speed camera. The dominant frequencies associated with flame oscillations are identified via fast-response pressure measurements. The present results show that there are two typical flame structures of triangle-shape and ellipse-shape found at relatively low and high fuel-to-air equivalence ratios respectively. The triangular flame at low equivalence ratios is mainly located in the shear layer of cavity flow and has small oscillations featured with low frequencies. At high fuel-to-air equivalence ratios, flame moves upstream and is anchored at the front edge of the cavity with elliptic shape and larger oscillations. The wall pressure distributions indicate that shock structures are formed in the isolator upstream of fuel injections at high equivalence ratios, leading to low speed flow in vicinity of fuel injections and causing flame move forward and change shape. Dominant frequencies from 49 Hz to 317 Hz are found for ethylene or mixture fuels. As fuel-to-air equivalence ratio increases, the dominant frequencies become smaller. For mixture fuel with hydrogen and methane, similar ignition process and flame structures are observed. However, the dominant frequencies related to flame oscillations for mixture fuels are not the same due to different combustion performance and thermal dissipation on turbulent flow.

1. Introduction

Supersonic combustion, as a key fundamental issue for hypersonic propulsion system, has drawn much attention of researchers for several decades. With ultrashort residence time for fuel at supersonic conditions, flame development and stabilization become very critical for combustion reliability and efficiency. Most of previous studies on flame of supersonic combustion are limited on hydrogen. There are very few reports of flame properties of hydrocarbon fuels at supersonic conditions. In recent years, hydrocarbons such as ethylene or methane have been considered potential fuel candidates for advanced propulsion systems [1,2]. Therefore, it is imperative to study flame characteristics of hydrocarbons in supersonic flows.

Meanwhile, for long-run supersonic combustor, thermal protection is another critical issue for reliable engine operation. Regenerative cooling using onboard fuel as coolant has been widely used [3], of which, hydrocarbon fuel such as aviation kerosene first flows through cooling channels in the engine structure and absorbs heat from the hot wall. As temperature rises, pyrolysis occurs and large molecules of fuel decompose into small molecules such as ethylene, methane. Many of previous studies of aviation fuel pyrolysis [4,5] have shown that the major products are hydrogen, ethylene and methane, totally accounting for more than 50% in molar fractions. For a regeneratively cooled supersonic combustor, before entering combustor, large molecular hydrocarbons have already been thermally cracked into small molecular hydrocarbons and hydrogen. Therefore, study of flame formation and propagation of mixture fuels of hydrocarbons and hydrogen is very necessary.

Flame characteristics are often studied by optical methods. For example, Micka et al. [6] applied CH*/OH* chemiluminescence to identify flame distribution and heat release rate in a Mach 2.2 supersonic combustor. Gruber et al. [7] studied combustion process of ethylene in a cavity-based supersonic combustor by taking luminescence photos of CH*/OH* and OH-PLIF images. Taguchi et al. [8] studied supersonic combustion of blended fuel of hydrogen and methane by using CH*/OH* chemiluminescence to observe flame structures and measuring wall pressure distribution to eval-

* Corresponding author at: State Key Laboratory of High Temperature Gas Dynamics, Institute of Mechanics, Chinese Academy of Sciences, Beijing 100190, China.
E-mail address: fzhong@imech.ac.cn (F. Zhong).
[1] These authors contributed equally to this work.

https://doi.org/10.1016/j.ast.2019.01.039
1270-9638/

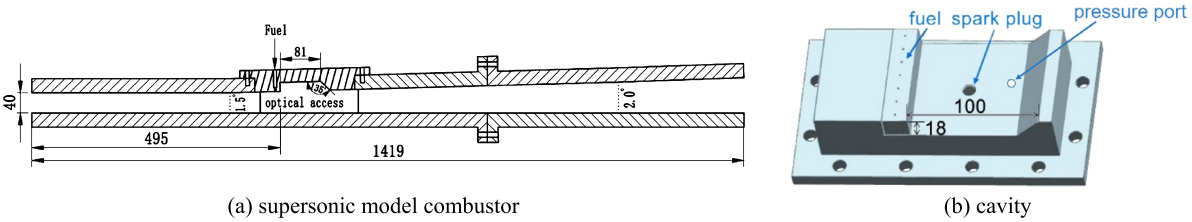

(a) supersonic model combustor (b) cavity

Fig. 1. Configuration of supersonic combustor with dimensions (unit: mm).

uate combustion performance. Tian et al. [9] investigated flame stability of a hydrogen and kerosene fueled combustor with an inflow condition of Mach number of 2 and static temperature of 656.5 K. Their results show that flame stability depends on fuel-to-air equivalence ratios of hydrogen and kerosene significantly. Fureby et al. [10] examined fuel/air mixing, self-ignition and flame stabilization of hydrogen fuel with varied kinds of strut injections in a supersonic crossflow experimentally and numerically. It is worthy noticing that most of previous studies are focused on flame zones after flame and combustion having been stabilized. Time evolution of flame from the very beginning of fuel ignition to flame propagation and then to flame stabilization has not been systematically studied yet.

In this paper, developments and structures of flame in a Mach 2.5 supersonic model combustor are studied with CH* chemiluminescence visualizations and fast-response pressure measurements. Ethylene is chosen as a basic fuel to study flame evolutions and associated frequencies at different fuel-to-air equivalence ratios. The mixture fuels of ethylene and hydrogen and of ethylene, methane and hydrogen are studied to investigate chemical effects of hydrogen and methane components on flame properties. The present work is aimed to provide detailed results of fuel ignition and flame development for better understanding of mechanisms of supersonic combustions.

2. Experimental setup

2.1. Experimental facilities and measurements

A direct-connect supersonic combustor is used and the combustor facility consists of an air heater, a nozzle and a combustor. The combination of air heater and nozzle can generate supersonic inlet flow with a total temperature of 1500–1900 K and a Mach number of 2.5. More details of the combustor facility can be found in our previous work [11,12]. Fig. 1(a) and (b) give schematic diagrams of the combustor section and the cavity component. As shown in Fig. 1, a cavity is used as a flame holder and several injection holes with an inner diameter of 2 mm are located 10 mm upstream of the cavity. A quartz window is installed on the combustor side walls as indicated in Fig. 1(a) for optical visualizations. The flame structures are illustrated by images of CH* chemiluminescence recorded by a camera with a frame speed of 10 000 fps and a resolution of 640 × 480. Wall pressures along the combustor axial direction are measured. A fast-response pressure transducer with a frequency resolution of 10 kHz is installed on the cavity floor as indicated in Fig. 1(b) to identify dominant frequencies of the combustor flow.

2.2. Fuels and experimental conditions

Table 1 lists four fuels with different compositions. For mixture fuels, components are well pre-mixed. The mass flow rate of each fuel is calibrated and controlled by orifice flow meter as described in our previous work [12]. For all the test cases, fuel-to-air equivalence ratio varies from 0.13–0.31 with an inlet total temperature of 1850 K (the temperature variation is less than ±30 K) and a Mach number of 2.5.

Table 1
Molar ratios of compositions of fuel (unit: %).

Fuel	H_2	CH_4	C_2H_4
A	/	/	100
B	20	/	80
C	20	30	50
D	20	40	40

Table 2
Fuel-to-air equivalence ratio (ϕ) of the test cases.

Case number/fuel type	1	2	3	4
A	0.14	0.17	0.21	0.30
B	0.13	0.17	0.24	0.31
C	0.13	0.17	0.27	0.31
D	0.13	0.17	0.23	0.31

For each test, air heater and nozzle first work for 2–3 s to generate a supersonic incoming flow with expected total temperature and Mach number. Then fuel is injected into combustor followed by ignition of spark plug after 0.1 s. The spark lasts for only 0.1 ms, which promotes ignition but does not affect flame development after that. Once fuel is ignited, flame starts to develop and propagate until being stabilized (in the view of time averaging) and the test runs for another 2 s before fuel is shut off and combustion ends.

2.3. CH* chemiluminescence and relative heat release rate

Chemiluminescence is often used as an indicator of flame structure as described in many of previous work [6,7]. For hydrocarbon fuels, chemiluminescence comes mainly from OH* and CH*. Compared to OH*, CH* has a much shorter life-time and is considered to be a better choice to illustrate flame structures. In the present study, luminosity of CH* is imaged by using ±15 nm bandwidth interference filters centered at a wavelength of 430 nm with a transmittance of 0.882. The instantaneous images of CH* are then recorded by a high-speed camera with a frame speed of 10 000 fps.

3. Experimental results and discussions

As mentioned before, the combustor inlet flow is kept the same with a total temperature of 1850 K and a Mach number of 2.5. Table 2 lists the fuel-to-air equivalence ratios of all the test cases. The fuel-to-air equivalence ratio is defined as the ratio of the mass flow rate of pure or blended fuels to the mass flow rate for the stoichiometric fuel-to-air ratio. The fuel/air equivalence ratio from 0.13 to 0.31 represents typical range of single injection stage for supersonic combustor.

It is found that for the same fuel-to-air equivalence ratio, the heating values for the four types of fuels as listed in Table 1 have small differences. With an air mass flow rate of 1 kg/s, the heating value of fuel A to D is 3.27 MW, 3.31 MW, 3.21 MW and 3.17 MW respectively. The maximum difference of heating value between the four fuels is less than 4.2%. However, ignition delay time for

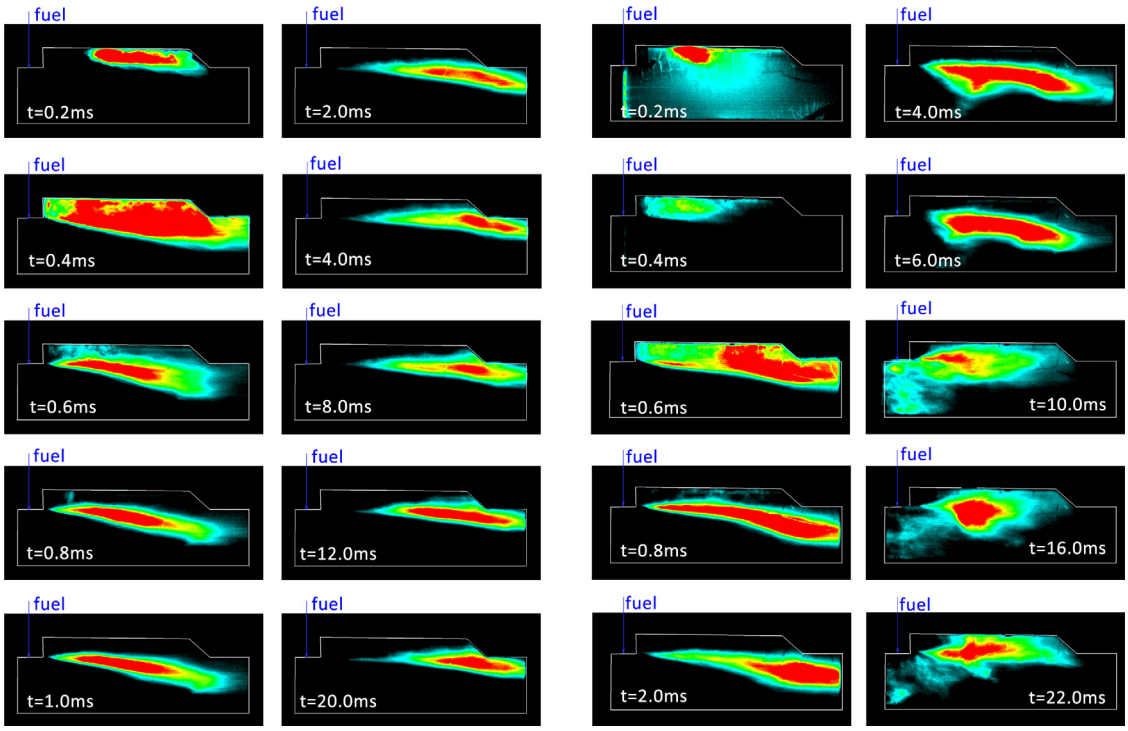

Fig. 2. Luminosity images of CH* during ethylene ignition.

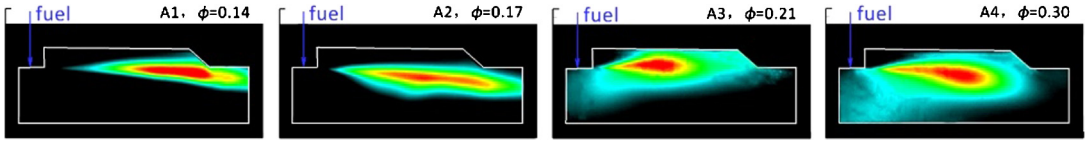

Fig. 3. Time averaged luminosity image of CH* for ethylene at four fuel-to-air equivalence ratios.

the four fuels is somewhat different. For example, for a typical value of fuel-to-air ratio equivalence ratio of 0.3 and at temperature and pressure of 1600 K and one atmosphere, the ignition delay time of fuel A to D is 0.028, 0.024, 0.036 and 0.044 ms, determined by a detailed kinetic mechanism of C2 proposed by Wang et al. [13]. Instead, laminar flame speed representing flame propagation properties for the four fuels is quite close to each other, that is 2.59, 2.61, 2.60 and 2.59 m/s.

3.1. Flame properties of ethylene

Ignition and flame formation of ethylene are first investigated. Fig. 2(a) shows instantaneous luminosity images of CH* (pseudo-color pictures) during the ignition process at a fuel-to-air equivalence ratio of 0.14 (case A1). The time of $t = 0$ denotes the beginning of spark ignition (it lasts for 0.1 ms). As shown in the figure, flame is initially generated on the cavity floor due to the spark effect. At $t = 0.4$ ms, the initial flame has already expanded in the whole cavity. As time advances, flame in the interior of the cavity disappears and it is mainly located in the cavity shear layer. From $t = 2$ ms, flame becomes quasi-steady with small oscillations in the streamwise direction. The flame oscillations would cause pressure fluctuations that are detected by fast-response pressure transducer as described lately. The flame development of ethylene at a fuel-to-air ratio of 0.17 (case A2) is very similar to that of case A1. Flame is initially generated in the cavity and then it spreads out. From a moment of $t = 2.0$ ms, flame is in a quasi-steady state accompany with back and forward oscillation with small amplitude.

As fuel-to-air equivalence ratio further increases, the flame development changes significantly. Fig. 2(b) is time evolution of flame at $\phi = 0.21$ (case A3). The initial flame is generated in the cavity and then is located in the shear layer of the cavity flow. However, flame is not stable in the cavity shear layer and it propagates upstream between $t = 2.0$ ms and 10.0 ms. The flame is anchored at the front edge of the cavity and located in the wake region of fuel jet from $t = 10.0$ ms. It will be shown later that for case A3, the time-averaged flame structure is quite different for that of case A1 and A2. The flame evolution of ethylene at $\phi = 0.3$ (case A4) is similar to that of case A3, which is mainly distributed in the jet wake region with large oscillations.

Fig. 3 gives time averaged luminosity image of CH* (10,000 samples with a total time of 1 s) to illustrate flame structures at four different fuel-to-air equivalence ratios. It is clearly shown that as fuel-to-air equivalence ratio increases, flame shape and distribution change significantly from a triangular shape located mainly in the cavity shear layer to an elliptical shape located mainly in the wake of fuel jet. The changes of shape and location of flame attribute to the fact that as more fuel is injected into the combustor, the shock structure is formed upstream of the fuel injections, which leads to lower flow speed in the vicinity of the injection site and accelerates fuel/air mixing and combustion.

The shock structure due to fuel injection and combustion can also be identified by plotting the wall pressure along the combustor axial direction. As shown in Fig. 4(a), at $\phi = 0.14$ and 0.17, wall pressure starts to rise downstream of the injections, indicating no shock waves are formed upstream of the injections and the incoming flow is supersonic. However, at $\phi = 0.21$, wall pressure

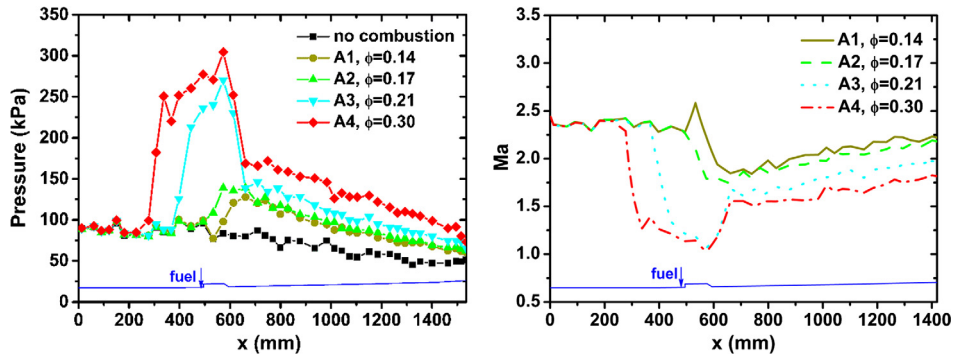

(a) wall pressure (b) Mach number

Fig. 4. Distribution of wall pressure and Mach number along the axial direction at varied equivalence ratios.

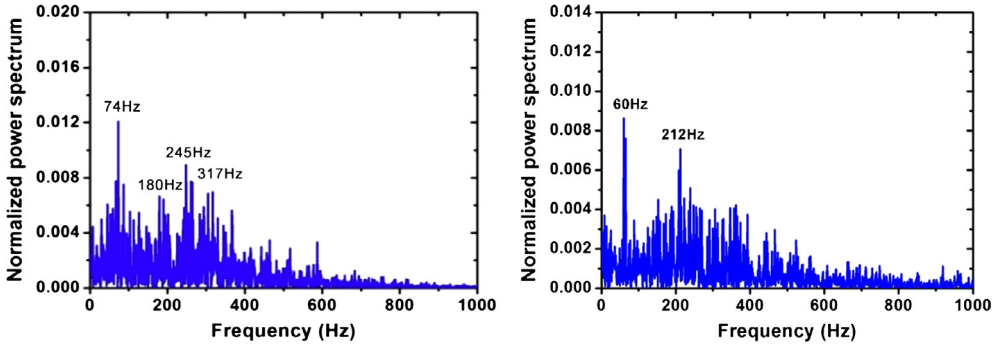

(a) Φ=0.14 (b) Φ=0.3

Fig. 5. Power spectrum of pressure signal for ethylene combustion at different equivalence ratios.

begins to rise approximately 150 mm upstream of the injections, caused by shock structures formed in the so-called isolator region to match the pressure difference between combustor inlet and the combustion zone as described in the study reported by Kobayashi et al. [14]. At $\phi = 0.3$, the wall pressure rise moves further upstream indicating a stronger shock structure in the isolator. Fig. 4(b) plots distribution of Mach number along the axial direction at varied fuel-to-air equivalence ratios. The Mach number, denoting the averaged value on cross sections of the combustor, is obtained by the measured wall pressures and the heat release rate determined by CH* luminosity images through a one-dimensional flow analysis based on mass, momentum and energy conservation laws as described in our previous work [12]. As shown in the figure, for the relatively high equivalence ratios ($\phi = 0.21$ and 0.3), the Mach number decreases upstream of the fuel injection indicating shock structures as described before.

The present study reveals an interesting phenomenon that dominant low frequencies are found for the present test cases and the frequency value changes with fuel-to-air equivalence ratios. Fig. 5(a) and (b) show results of power spectrum of pressure signal measured by fast-response pressure transducer mounted on the cavity floor. It is clearly shown that for both test cases (A1 and A4), relatively low frequencies are observed. For $\phi = 0.14$, the dominant frequencies are 74 Hz and 245 Hz, and for $\phi = 0.3$, the dominant frequencies decrease to 60 Hz and 212 Hz. It is believed that the relatively low frequencies of a few hundreds of Hz or less are related to thermo-acoustic instability caused by interactions of heat release and turbulent jet flow of fuel, which has been studied by Lin, Ma and Yang [15] and by Wang, Sun et al. [16]. The acoustic waves that are formed by fuel injection and propagate downstream would be reflected at a location where local thermal throat is caused by chemical heat release. Then the acoustic waves would transport upstream and affect the fuel injection and fuel/air mixing. With a feedback loop of acoustic waves as described above, the flame oscillation occurs with certain dominant frequencies.

3.2. Effect of hydrogen addition

Fig. 6(a) gives images of CH* luminosity for fuel B of 80% ethylene and 20% hydrogen at $\phi = 0.13$ (case B1). The evolution of flame is almost the same as that of ethylene at $\phi = 0.14$ (case A1) with flame initially growing and spreading in the cavity and finally being stabilized in the cavity shear layer with small oscillations. Fig. 6(b) is the result for $\phi = 0.31$ (case B4). The flame is not stabilized in the shear layer flow of the cavity, instead, it moves upstream and is located in the jet wake region with relatively large oscillations.

Fig. 7 gives the time averaged luminosity of CH* (pseudo-color pictures) for fuel B at varied equivalence ratios. At low value of ϕ, a triangle-shaped flame structure is observed. As ϕ increases, flame appears in a typical elliptic shape and it is anchored at the front edge of the cavity and distributed in the jet wake region.

Fig. 8(a) and (b) give power spectrum of pressure fluctuations for fuel B at two typical equivalence ratios. For case B1 with $\phi = 0.13$, the most dominant frequency is 69 Hz, which is slightly smaller than that of case A1 (74 Hz). The reduction of dominant frequency is expectable since for fuel B with hydrogen addition, combustion efficiency is higher in the cavity region resulting in more heat releasing and stronger damping on turbulence fluctuations. For case B4 with $\phi = 0.31$, the most dominant frequency is found to be 49 Hz, which is also lower than that of case A4 with a value of 60 Hz.

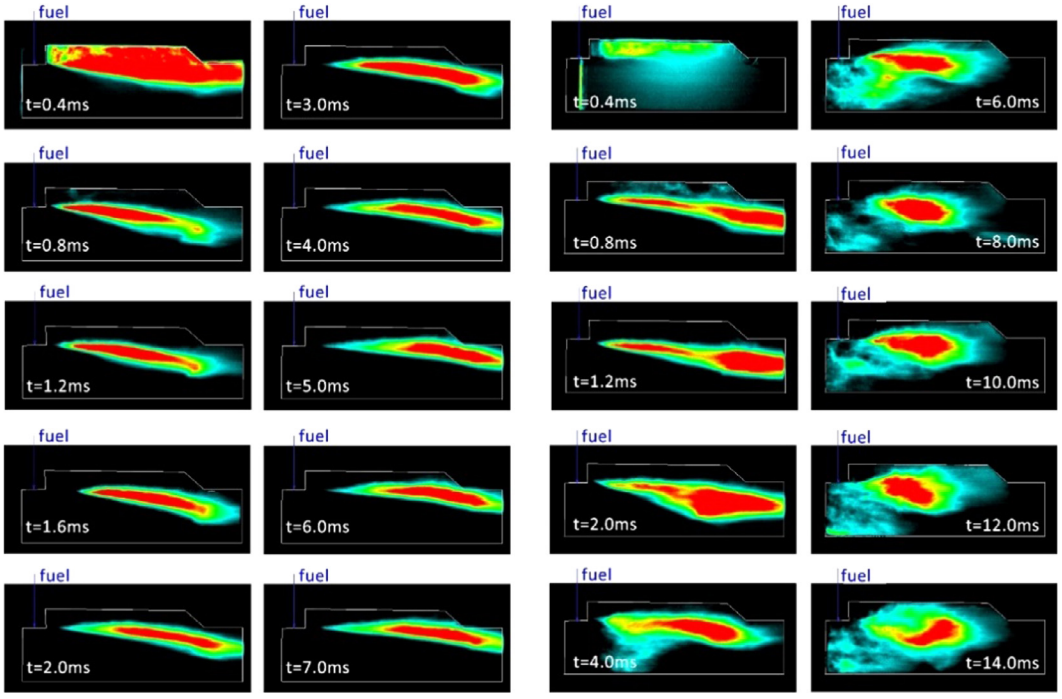

(a) Φ=0.13 (b) Φ=0.31

Fig. 6. Luminosity images of CH* of ignition of mixture fuel B ignitions.

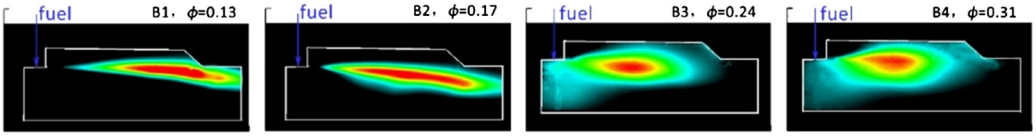

Fig. 7. Time averaged luminosity image of CH* for fuel B at different equivalence ratios.

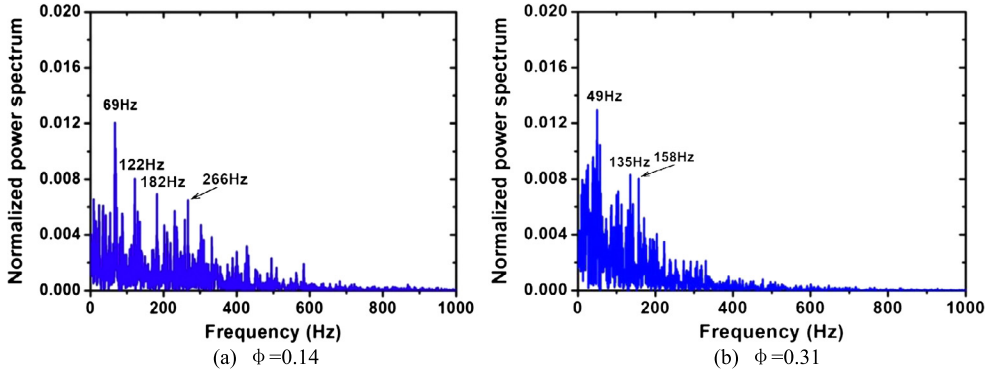

(a) Φ=0.14 (b) Φ=0.31

Fig. 8. Power spectrum of pressure signal for fuel B at different equivalence ratios.

3.3. Effect of methane addition

Fuel C and D are fuel mixture with methane. Fuel C consists of 20% hydrogen, 50% ethylene and 30% methane, and fuel D is 20% hydrogen, 40% ethylene and 40% methane.

The ignition time defined as the time from the beginning of plug sparking to the moment when flame reaches a quasi-steady state for varied types of fuel and fuel-to-air equivalence ratios are plotted in Fig. 9. It can be seen that for all the four types of fuel, the ignition time increases overall with fuel-to-air equivalence ratios and at a middle value of equivalence ratio, the ignition time increases suddenly with a large extent. It may attribute to the fact that at a middle value of fuel-to-air ratio, flame formation and stabilization changes from cavity shear layer stability to wake stability

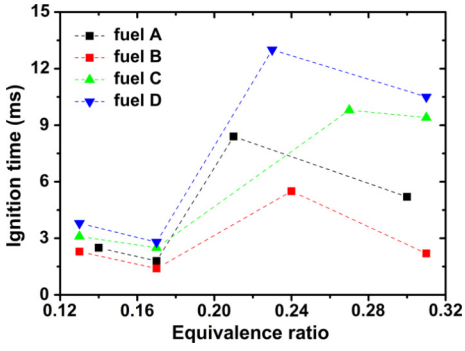

Fig. 9. Change of ignition time of the four fuels as a function of fuel-to-air equivalence ratio.

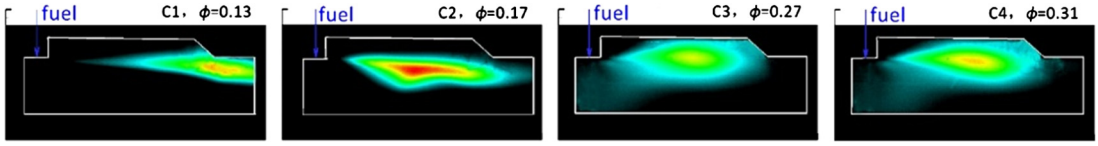

Fig. 10. Time averaged luminosity image of CH* for fuel C at four fuel-to-air equivalence ratios.

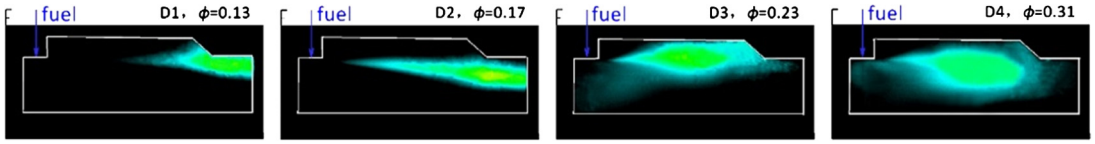

Fig. 11. Time averaged luminosity image of CH* for fuel D at four fuel-to-air equivalence ratios.

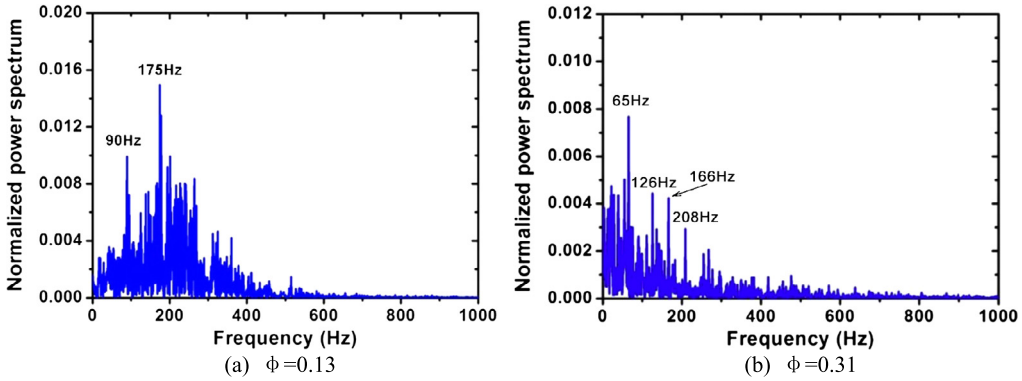

Fig. 12. Power spectrum of pressure signal for fuel C combustion at different equivalence ratios.

of fuel jets as discussed before. At the same time, it is found with hydrogen addition, the ignition time of fuel B is the smallest. However, the ignition time of fuel D is the longest due to the largest fraction of methane.

The instantaneous images of CH* luminosity of fuel C and fuel D reveal similar ignition processes compared to that of fuel A and B. There also exist two typical flame structures (triangular and elliptical). Fig. 10 and Fig. 11 show the time-averaged CH* luminosity for fuel C and D. The typical slender triangle-shape and ellipse-shape flames are observed at $\phi = 0.13$ and $\phi = 0.31$. An interesting phenomenon is that for fuel C at $\phi = 0.17$, a transition state of flame with a wide triangle shape is observed.

Fig. 12(a) and (b) give the power spectrum of pressure fluctuations for fuel C at $\phi = 0.13$ and $\phi = 0.31$. A comparison of Fig. 5 and Fig. 12 clearly shows that the dominant base frequency of fuel C at both low and high equivalence ratios is higher than that of fuel A. The reason is that with methane addition, combustion and heat release of fuel C are less effective than those of fuel A and turbulence dissipation due to thermal effects becomes weaker.

4. Conclusions

In this paper, flame characteristics of ethylene and mixture fuels in ignition process in a Mach 2.5 supersonic model combustor are studied and typical flames structures and associated dominant frequencies are identified. Below are few conclusions in terms of the present results.

1) Ignition process of ethylene and mixture fuels of ethylene, hydrogen and methane are found quite similar, of which, initial flame is generated near the cavity floor and expanses in the cavity. After 0.6–0.8 ms from spark ignition, the flame is located in the shear layer of the cavity flow. However, for relatively large fuel-to-air equivalence ratios, the flame in the cavity shear layer is not stable and it moves upstream and is relocated in the wake region of the fuel jet.

2) There are two typical flame structures of triangle-shape and ellipse-shape found at low and high fuel-to-air equivalence ratios respectively. The triangular flame at low equivalence ratios is mainly located in the shear layer of cavity flow and has small oscillations. At high equivalence ratios, flame moves upstream and anchored at the front edge of the cavity with elliptic shape and larger oscillations.

3) The wall pressure and the averaged Mach number distributions indicate that shock structures are formed in the isolator at high equivalence ratios, leading to low speed (low Mach number) flow in vicinity of fuel injections and changes in flame shape.

4) Characteristic frequencies from 49 Hz to 317 Hz are found for ethylene or mixture fuels. As fuel-to-air equivalence ratio increases, the dominant frequencies become smaller.

5) For mixture fuels with hydrogen and methane, similar ignition process and flame structures are observed. However, the dominant frequencies related to flame oscillations are not the same due to different amount of heat release and thermal dissipation on turbulent flow.

Conflict of interest statement

There is no conflict of interest.

Acknowledgement

This work is supported by the National Natural Science Foundation of China (Grants 91441102 and 11672307) and Youth Innovation Promotion Association, Chinese Academy of Sciences.

References

[1] J.M. Tishkoff, J.P. Drummond, T. Edwards, A.S. Nejad, AIAA Paper 1997-1017, 1997.

[2] A.M. Storch, M. Bynum, J. Liu, M. Gruber, AIAA Paper 2011-2249, 2011.
[3] H. Huang, L. Spadaccini, D. Sobel, J. Eng. Gas Turbines Power 126 (2) (2004) 284–293.
[4] F.Q. Zhong, X.J. Fan, G. Yu, J.G. Li, C.J. Sung, J. Thermophys. Heat Transf. 25 (2) (2011) 450–456.
[5] X.J. Fan, F.Q. Zhong, G. Yu, J.G. Li, C.J. Sung, J. Propuls. Power 25 (6) (2009) 1226–1232.
[6] D.J. Micka, J.F. Driscoll, Proc. Combust. Inst. 32 (2) (2009) 2397–2404.
[7] M.R. Gruber, J.M. Donbar, C.D. Carter, K.Y. Hsu, J. Propuls. Power 20 (5) (2014) 769–778.
[8] H. Taguchi, S. Tomioka, H. Nagata, M. Kono, J. Jpn. Soc. Aeronaut. Space Sci. 42 (483) (1994) 224–231.
[9] Y. Tian, S.H. Yang, J.L. Le, Aerosp. Sci. Technol. 59 (2016) 183–188.
[10] C. Fureby, K. Nordin-Bates, K. Petteson, A. Bresson, V. Sabelnikov, Proc. Combust. Inst. 35 (2015) 2127–2135.
[11] L.W. Cheng, F.Q. Zhong, H.B. Gu, X.Y. Zhang, Int. J. Heat Mass Transf. 96 (2016) 249–255.
[12] Z.P. Wang, H.B. Gu, L.W. Cheng, F.Q. Zhong, X.Y. Zhang, Int. J. Turbo Jet-Engines (2016), ISSN (Online) 2191-0332.
[13] H. Wang, A. Laskin, Z.M. Djurisic, C.K. Law, S.G. Davis, D.L. Zhu, in: 1999 Fall Technical Meeting of the Eastern States Section of the Combustion Institute, Raleigh, NC, 1999, pp. 129–132.
[14] K. Kobayashi, S. Tomioka, K. Kato, A. Murakami, K. Kudo, J. Propuls. Power 22 (3) (2006) 518–526.
[15] K.C. Lin, F. Ma, V. Yang, J. Propuls. Power 26 (6) (2010) 1161–1169.
[16] Z.G. Wang, M.B. Sun, H.B. Wang, J.F. Yu, J.H. Liang, F.C. Zhuang, Proc. Combust. Inst. 35 (2015) 2137–2144.